# Block Copolymer Self-Assembly Induced Compatibilization of PCL/PS−PEP Blends

**Rong-Ming Ho* and Yeo-Wan Chiang**

*Department of Chemical Engineering, National Chung-Hsing University, Taichung 40227, Taiwan, R.O.C.*

**Chu-Chien Lin**

*Department of Chemistry, National Chung-Hsing University, Taichung 40227, Taiwan, R.O.C.*

**S. J. Bai**

*Institute of Materials Science and Engineer, National Sun Yet-Sen University, Kaohsiung 804, Taiwan, R.O.C.*

*Received August 2, 2001; Revised Manuscript Received November 5, 2001*

ABSTRACT: An interesting way to obtain compatible blends of poly(ϵ-caprolactone) (PCL) and polystyrene-*b*-poly(ethylenepropylene) (PS−PEP) has been achieved. The intrinsically immiscible blends such as PCL/PS and PCL/PEP become compatible while the PS and PEP components form a diblock copolymer to melt blending with PCL. The morphology of PCL/PS−PEP blends was examined by polarized light microscopy, small-angle X-ray scattering, and transmission electron microscopy (TEM). The PCL/PS−PEP blends were found to self-assemble as lamellar microstructure with tens of nanometers dimension. Their compatibilities were investigated in terms of differential scanning calorimetry. No significant change on the $T_g$ of PEP-rich phase in the blends has been found whereas the $T_g$ of PS-rich phase gradually decreases with decreasing the molecular weight of PCL in blends. However, the changes on the $T_g$ of PS are insignificant as compared to the expected glass transition temperature predicted by the Fox equation. Taking advantage of the driving force of self-assembly for block copolymers, the PCL component appears to be localized in between the lamellar microdomains of PS block. The behavior of localization for PCL was further confirmed by the TEM phase contrast imaging. Contrary to typical microphase-separated morphology of crystallizable block copolymers (designated as chemically confined environment for crystallizing blocks), we name this unique phase-separated morphology as a physically confined environment for the crystallization of PCL.

## Introduction

Aliphatic polyesters represent an important family of biodegradable materials.[1−7] Increasing attention has been focused on hydrolytically unstable lactone polymers owing to their biomedical applications. Copolymerization and blending with aliphatic polyesters have been used to modify raw polymeric materials for biodegradation. Blending processes might offer a more cost-effective way than chemical modification. However, most of the blends were found to be immiscible. Macrophase separation with separated domain size above submicron is usually observed so as to depress the effect of modification for biodegradation. Here, we found an interesting way to obtaining compatible blends from the blending of poly(ϵ-caprolactone) (PCL) and polystyrene-*b*-poly(ethylenepropylene) (PS−PEP). The intrinsically immiscible blend systems such as PCL/PS[8−10] and PCL/PEP[11] become compatible while the PS and PEP form a diblock copolymer to be melted blending with PCL.

For the ordinary blends of homopolymer A and block copolymer A−B such as homopolymer PS and styrenic block copolymer, the occurrence of macrophase separation (i.e., the solubility limit) is strongly dependent upon the ratio of the molecular weight of homopolymer A ($M_{AH}$) to the A block of copolymer ($M_{AC}$). Systematic studies with regard to the phase behavior of homopolymer A/block copolymer A−B blending systems have been well explored up to now.[12−23] These studies conclude that the homopolymer A tends to be selectively solubilized in the A microdomains of block copolymer while the value of $M_{AH}/M_{AC}$ is less than one. Owing to the change in interfacial area per block, the solubilization might lead to the transformation of microstructure. Macrophase separation of homopolymer occurs while the value of $M_{AH}/M_{AC}$ is larger than one. If the value of $M_{AH}/M_{AC}$ is equal to one, a unique morphology having homopolymer localized in the middle of the A microdomains of block copolymer has been observed. The occurrence of microstructure transformation is thus absent due to the insignificant change on the interfacial area between the A and B microdomains. Contrary to the phase behavior of A/A−B blends, remarkably different phase behavior has been found in the PCL/PS−PEP blending system (i.e., C/A−B blends). A new mechanism of compatibilization, block copolymer self-

**Table 1. Ring-Opening Polymerization of Lactones[24]**

| code | $M_n$(obsd)[a] | $M_w/M_n$ | $M_n$(calcd)[b] |
|---|---|---|---|
| PCL3 | 2 800 | 1.12 | 1 425 |
| PCL5 | 4 500 | 1.06 | 2 850 |
| PCL11 | 11 000 | 1.10 | 5 700 |
| PCL19 | 19 100 | 1.08 | 11 400 |
| PCL44 | 43 900 | 1.15 | 22 800 |

[a] Obtained from SEC analysis. [b] Calculated from the molecular weight of lactone times moles. For details of the measurement and calculation, see our previous publication.

* To whom all correspondence should be addressed. Tel 886-4-2857471; Fax 886-4-2854734; e-mail rmho@dragon.nchu.edu.tw.

10.1021/ma011381j CCC: $22.00 
Published on Web 01/15/2002

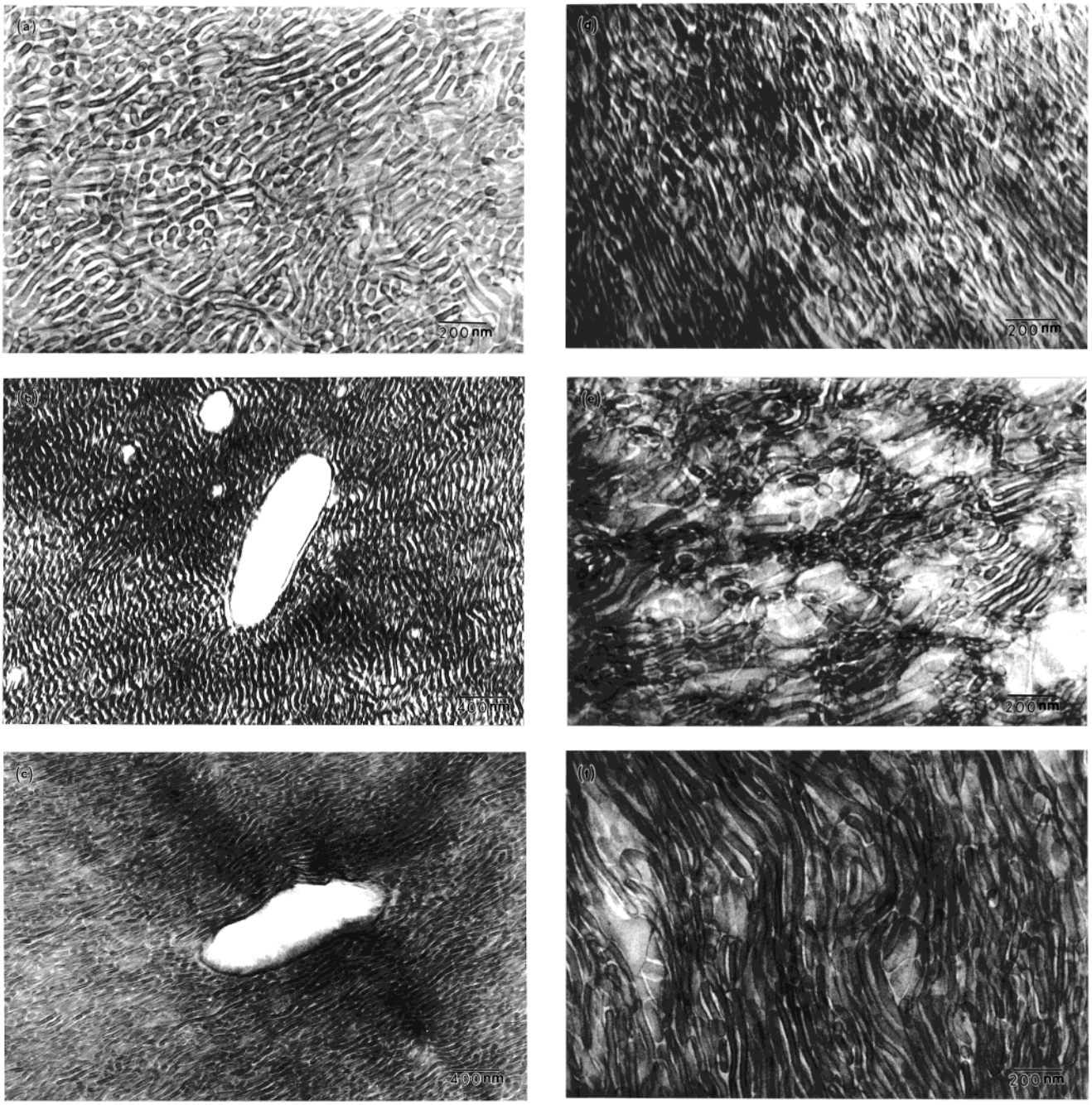


**Figure 1.** TEM micrographs of microsectioned (a) PS−PEP, (b) PCL44/PS−PEP blends, (c) PCL19/PS−PEP blends, (d) PCL11/PS−PEP blends, (e) PCL5/PS−PEP blends, and (f) PCL3/PS−PEP blends by mass thickness contrast.

assembly induced compatibilization, is proposed for the compatible blends of PCL/PS−PEP in this study.

## Experimental Section

**Materials.** The styrenic triblock copolymer used in this investigation is a diblock copolymer of polystyrene-*block*-poly(ethyleneepropylene) symbolized as PS−PEP (Kraton G1701 of Shell Co.). According to the supplier, this commercial PS−PEP possesses 37 wt % styrene content. Size exclusion chromatography (SEC) indicated that the number-average molecular weight, $M_n$, of as-supplied PS−PEP is ca. 211 000 g/mol, and the polydispersity index is ca. 1.12. Various poly($\epsilon$-caprolactone) (PCL) samples with narrow polydispersity index (Table 1) were synthesized in terms of living and immortal polymerization of lactones catalyzed by a novel aluminum alkoxide. The detailed synthetic routes were described in our previous paper.[24]

**Blending Processes.** Melt-mixed samples were prepared in a MiniMax mixer. The MiniMax mixing cup was preheated to 250 °C, and 0.15 g of the PCL powder and 0.85 g of PS−PEP powder were simultaneously introduced. Each blend was melt processed at 250 °C for 10 min at 400 rpm. The mixer was purged with industrial grade nitrogen gas before loading to reduce degradation; blending was done under a nitrogen blanket. During mixing, the rotor plate was raised intermittently every several minutes to promote more efficient mixing. After processing, the samples were quenched by ice water. It is noted that there is no significant change in the molecular weights of the PCL and PS−PEP for these samples after melt-mixed process as evidenced by SEC measurements. This result suggests that degradation of PCL and PS−PEP during processing is minimized.

**Microscopy.** Thin films of the blends having thickness of micron range and of tens of nanometers for polarized light microscopy (PLM) and transmission electron microscopy (TEM)

observations, respectively, were obtained by ultra-cryomicrotomy using a Reichert Ultracut microtome (equipped with a Reichert FCS cryochamber and a diamond knife). All of the samples prepared by cryomicrotomy were operated at −120 °C. The PLM image was obtained by an Olympus BX60 polarized light microscope installed with a DP10 digital camera. Bright field TEM images were obtained by the phase contrast on a JEOL JEM-1200x transmission electron microscope at an accelerating voltage of 120 kV. Staining was accomplished by exposure the samples to the vapor of a 4% aqueous $RuO_4$ solution for 30 min. Bright field TEM images of mass−thickness contrast were obtained from the stained samples.

**Small-Angle X-ray Scattering (SAXS).** SAXS experiments were conducted at the synchrotron X-ray beam-line X27C at the National Synchrotron Light Source in Brookhaven National Laboratory. The wavelength of the X-ray beam is 0.1307 nm. The zero pixel of the SAXS patter was calibrated using silver behenate, with the first-order scattering vector $q^*$ ($q^* = 4\pi\lambda^{-1} \sin\theta$, where $2\theta$ is the scattering angle) being 1.076 $nm^{-1}$.

**Differential Scanning Calorimetry (DSC).** DSC experiments were carried out in a Seiko DSC 220C and a Perkin-Elmer DSC 7 for the measurements of low-temperature range (i.e., the $T_g$ measurements of PEP-rich and PCL phases) and high-temperature range (i.e., the $T_g$ measurements of PS-rich phase), respectively. The temperature and heat flow scales at different heating rates were carefully calibrated using standard materials. The samples were first heated to the maximum annealing temperature, $T_{max} = 140$ °C, for 5 min to eliminate the PCL crystalline residues formed during the preparation procedure. For the $T_g$ measurements of PEP-rich and PCL phases, the polymer samples were then quenched by liquid nitrogen and immediately transferred to DSC chamber at preset temperature −140 °C in order to prevent the occurrence of crystallization during cooling. For the $T_g$ measurements of PS-rich phase, the polymer samples were then quenched by a rate of 150 °C/min to generate amorphous glassy samples. Consecutive heating was performed at heating rates of 10 °C/min. The DSC sample size was 10−15 mg.

## Results and Discussion

**Morphology of PCL/PS−PEP Blends.** The morphology of PS−PEP microstructure after melt processing is shown in Figure 1a. The morphological observation demonstrates that the diblock copolymer of PS−PEP self-assembles to form lamellar microstructure. The microdomains of PS component appear relatively dark after staining by $RuO_4$, while the microdomains of PEP component appears light. SAXS results further confirmed the observed lamellar microstructure where the scattering peaks occurred at $q^*$ ratio of 1:2:3:4 (Figure 2a). The long period of lamellae was determined as 60.0 nm. Different morphological textures were obtained while 15 wt % amount of various PCL species having a wide variety of molecular weight was introduced to the matrix of PS−PEP. Dispersed domains (bright area in picture) with submicron size are obtained after the introduction of high molecular weight PCL components as illustrated in Figure 1b,c. These macrophase-separated microdomains are identified as PCL-rich phase by PLM observations where the crystallizing PCL component shows typical character of birefringence. The microstructure of microphase-separated copolymer still appears lamellar texture with slight change in long period ($d$-spacing = 61.0 nm for PCL44/PS−PEP blends) as identified by SAXS measurement. Most surprisingly, there are no significant dispersed macrodomains observed in the blends containing low molecular weight PCL components (Figure 1d−f). Lamellar microdomains are recognized. SAXS results confirmed the observed lamellar microstructure for the compatible blends as illustrated in Figure 2b,c. It is interesting to find that the long period of the blends was much larger than the value of neat copolymer. For instance, the long period of lamellae was determined as 69.5 nm for PCL3/PS−PEP. This significant change in long period is attributed to the specific phase behavior, the localization behavior of PCL (see below for reasons).

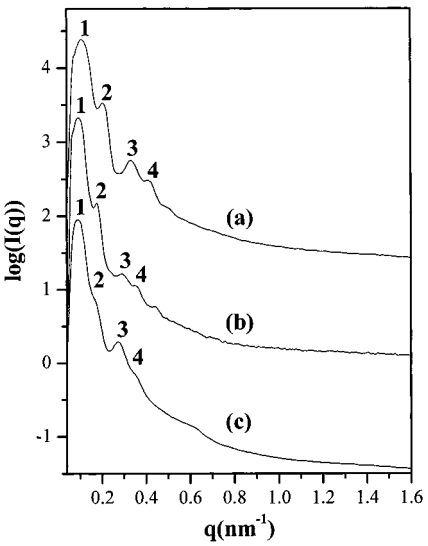


**Figure 2.** One-dimensional (1D) SAXS profiles of (a) PS−PEP, (b) PCL11/PS−PEP blends, and (c) PCL3/PS−PEP blends.

**Localization of PCL.** The solubility parameters of the PS block, the PEP block, and the PCL component are determined as 9.04, 7.88, and 9.57 $(cal/cm^3)^{1/2}$, respectively, as estimated from the structural formula and the densities of the compounds using Small's method.[25] The densities of the PS block, the PEP block, and the PCL component are 1.05,[26] 0.86,[27] and 1.08 $g/cm^3$, respectively. It is noted that the discrepancy in solubility parameters between PCL ($\delta$ = 9.57 $(cal/cm^3)^{1/2}$) and PS ($\delta$ = 9.04 $(cal/cm^3)^{1/2}$) is much smaller than the difference between PCL and PEP ($\delta$ = 7.88 $(cal/cm^3)^{1/2}$). It is reasonable to presume that the PCL component is the favor of the PS block instead of the PEP block. We thus deduce that the PCL component is either mixed with the PS block or located in between the lamellar microdomains of the PS block as illustrated in Figure 3. The morphological textures have been found in different homopolymer/copolymer blends such as homopolymer PS/polystyrene-*b*-polyisoprene (SI) diblock copolymer[28,29] and homopolymer poly(α-methylstyrene) (PαMS)/polystyrene-*b*-polybutadiene−polystyrene (SBS) triblock copolymer mixtures.[30] The first instance was designated by Hashimoto and co-workers as the behavior of solubilization for homopolymer in block copolymer, whereas the later instance was designated as the behavior of localization.[28,29] To further identify the formed texture of PCL/PS−PEP, blends were examined by differential scanning calorimetry (DSC). The $T_g$'s of various PCL samples determined are in the vicinity of −60 °C; the $T_g$ value is independent of molecular weight (Figure 4). Figure 5 shows the DSC thermograms of various PCL/PS−PEP blends. No significant change has been found in the $T_g$ of PEP-rich phase in all of the blends studied. As illustrated in Figure 5a, the $T_g$ transition trace of neat PS−PEP is almost alike to that of PCL3/PS−PEP blends. In contrast to the $T_g$ behavior

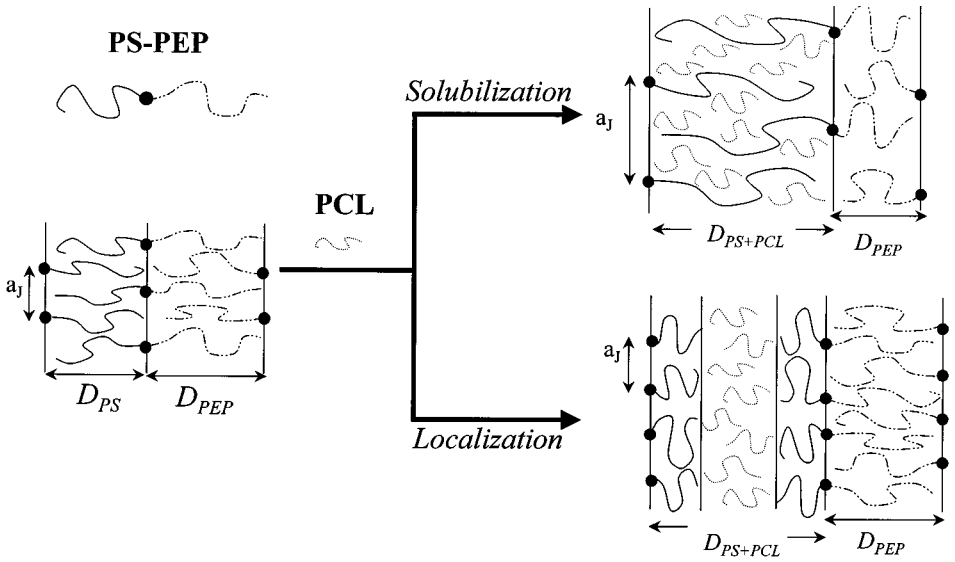


**Figure 3.** Schematic diagram of the behavior of localization and the solubilization of PCL in PS−PEP block copolymer matrix. $D$ and $a_j$ represent the domain dimension of lamellar layer and the average distance between the chemical junction, respectively.

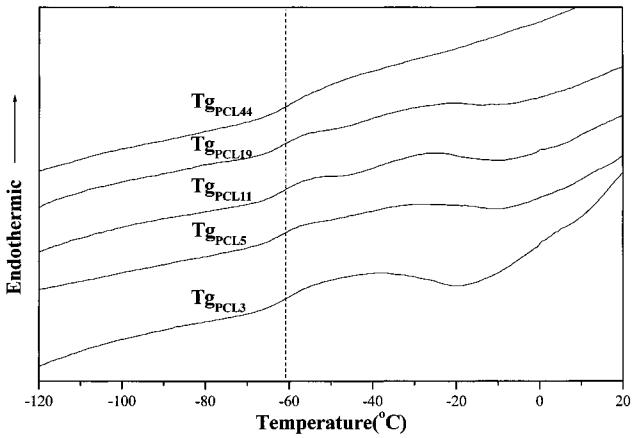


**Figure 4.** DSC thermograms of various PCL homopolymers having different molecular weight. The heating rate is 10 °C/min for all the scans.

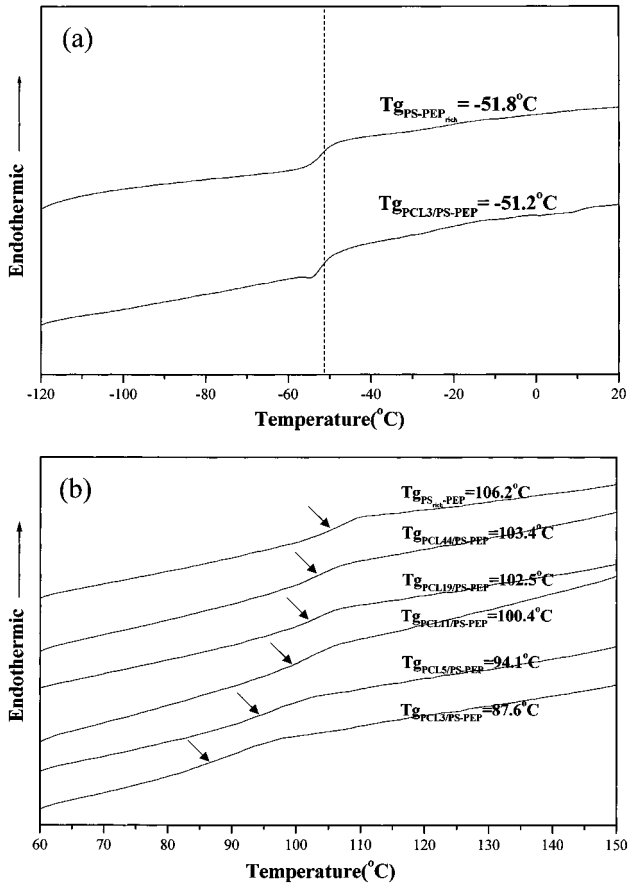


**Figure 5.** DSC thermograms of various PCL/PS−PEP blends at (a) lower temperature range and (b) higher temperature range. The heating rate is 10 °C/min for all the scans.

of PEP-rich phase in blends, the $T_g$ of PS-rich phase gradually decreases with decreasing the molecular weight of PCL in blends (Figure 5b). This reflects that the PCL component is indeed of favor PS segments as suggested previously. Furthermore, the changes in the $T_g$ of PS are insignificant as compared to the predicted glass transition temperature (ca. 27 °C) from the derivation of Fox equation (Figure 6a). For instance, the content of PCL solubilized in the PS-rich microdomains of PCL3/PS−PEP blends (the blends with the highest degree of PCL solubilization) was estimated to be less than 15 wt % of total amount PCL added. The results of $T_g$ measurements are consistent with previous morphological observations where the occurrence of microstructure transformation is absent. Essentially, microstructure transformation is expected for the PCL/PS−PEP compatible blends having the added amount of PCL solubilized in PS−PEP. On the basis of the microstructure observation (i.e., no phase transformation) and the insignificant change on the $T_g$ of PS-rich phase, we suggest that the majority of PCL component is localized in between the lamellar microdamains of PS block. Namely, the localization of PCL dominates the behavior of solubilization while the PCL/PS−PEP blends are compatible. The suggested phase behavior was further identified by the SAXS results (Figure 6b). The long period determined by SAXS significantly increases once the blends become compatible. Furthermore, the change on the long period is almost invariant disregarding the molecular weight of PCL added. Also, the increase in long period is about 15% of the original dimension. This increase is nearly equal to the amount of PCL added in the blends. It is evident to indicate that the majority of PCL is localized in between the lamellar microdamains

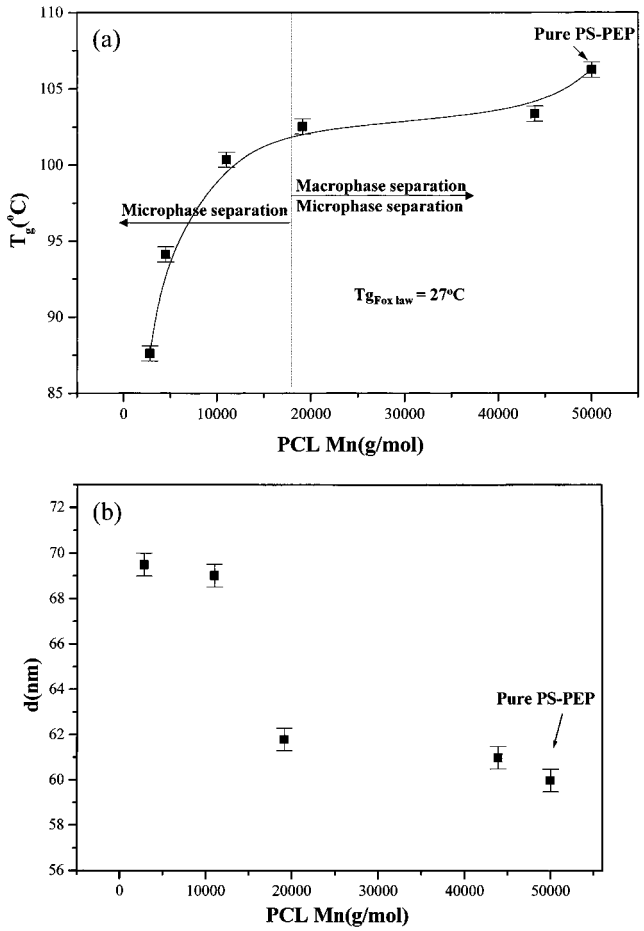


**Figure 6.** PCL molecular weight dependence of (a) glass transition temperatures and (b) long periods for PCL/PS−PEP blends. The solid line in the plot is the guiding line for phase behavior.

of PS block so as to extensively swell the lamellar microdomain in the direction of lamellar normal. As a result, the phase behavior is dependent upon the molecular weight of PCL. Increasing the molecular weight of PCL decreases the occurrence of solubilization and localization so as to persuade macrophase separation (Figure 6a).

The suggested morphology might be further confirmed in terms of TEM observations by phase contrast imaging. For neat PS−PEP without staining, the microdomains of PS component appear relatively dark under TEM by phase contrast at suitable underfocus owing to the effects of mean inner potential difference as described by Thomas and co-workers,[27] whereas the microdomain of the PEP component appears light (Figure 7a). As observed, phase-separated PCL from PS−PEP matrix presents bright domains under TEM by phase contrast. Figure 7b illustrates one of the typical TEM micrographs for the compatible blends of PCL/PS−PEP. In contrast to the imaging of mass thickness contrast (Figure 1e), a much clear morphological texture is obtained by the phase contrast imaging owing to the discernible contrast between the PS-rich and PCL-rich microdomains. A schematic diagram to illustrate the observed morphology is given in Figure 7c. The larger PCL-rich microdomains exhibit bright area in contrast to the dark area of the PS-rich phase although those smaller PCL-rich microdomains is difficult to be identified due to the resolution limitation of imaging. Nevertheless, the irregularly swelling microdomains (the bright area) can be recognized. Therefore, we suggest that the formation of these irregularly swelling microdomains is the result of PCL aggregations. The morphology of the irregularly swelling microdomains of PCL in PCL/PS−PEP blends is similar to the nonuniformly distributed microdomains of PαMS in PαMS/SBS blends studied by Hashimoto and coworkers.[30] They suggested that the balance of two opposing physical factors in Gibbs free energy of mixing: loss of combinatorial entropy of PαMS and reduction of interaction energy (i.e., reduction in the interfacial area) between the PαMS and the PS is responsible for the formation of this unique microstructure. In other words, the irregular swelling (i.e., nonuniform distribution of PαMS perpendicular and parallel to the interface of microdomains) is attributed to the behavior of localization combined with the repulsive interaction between the PαMS and the PS. Our morphological results of PCL/PS−PEP are consistent with above thermodynamic interpretations (see below in detail).

**Block Copolymer Self-Assembly-Induced Compatibilization.** As observed, the homopolymer PCL is either localized in between the lamellar microdomains of PS block to form tens of nanometer-scale microdomains or phase-separated from PS−PEP to form around submicron size domains. For typical blending system (A/A−B blends), the solubility limit occurs at the blends of that $M_{AH}/M_{AC}$ is larger than one. Contrary to the A/A−B blends, the value of $M_{PCL}/M_{PS}$ for PCL/PS−PEP blends where macrophase separation occurs is ca. 0.24 based on the results of SEC molecular weight measurements. Furthermore, there is very minor possibility to form completely solubilized phase containing PCL component and PS block as evaluated by DSC measurements. Obviously, the phase behavior of self-assembly PCL/PS−PEP blends is much more complicated than the behavior of A/A−B blends.

The morphological results and the compatibility studies reflect that the formation of phase-separated domains of PCL from PS−PEP matrix is strongly dependent upon their molecular weight. It is reasonable to infer that the compatibilization is the results of entropic origin. However, it has been identified that the polymer pairs of PCL/PS and PCL/PEP are intrinsically immiscible. The influence of entropic effect is not as significant as enthalpic penalty to dominate the miscibility. Even for the use of oligomeric PCL, the polymer pair of PCL/PS has been found to form macrophase separation. The polymer pair of PCL/PEP is even not possible to possess miscibility since the interaction parameter of PCL and PEP ($\chi_{PCL/PEP}$) is even larger than the interaction parameter of PCL and PS ($\chi_{PCL/PS}$). The morphological results lead to the question, what are the origins of the compatibilization for PCL/PS−PEP blends? One of the possible interpretations is ascribed to the formation of smaller phase-separated domains as the result of processing effect. To alleviate the influence of processing, melt-blending samples have been further annealed at temperature above the $T_g$ of PS (the highest $T_g$ of constituent components in blends) for more than 1 week. The majority of sample area remains lamellar texture, but there exists much significant behavior of irregularly swelling as shown in Figure 8. The occurrence of macrophase separation is still absent after extensive annealing. These results indicate that the melt-mixed morphology is dominated by thermodynamic

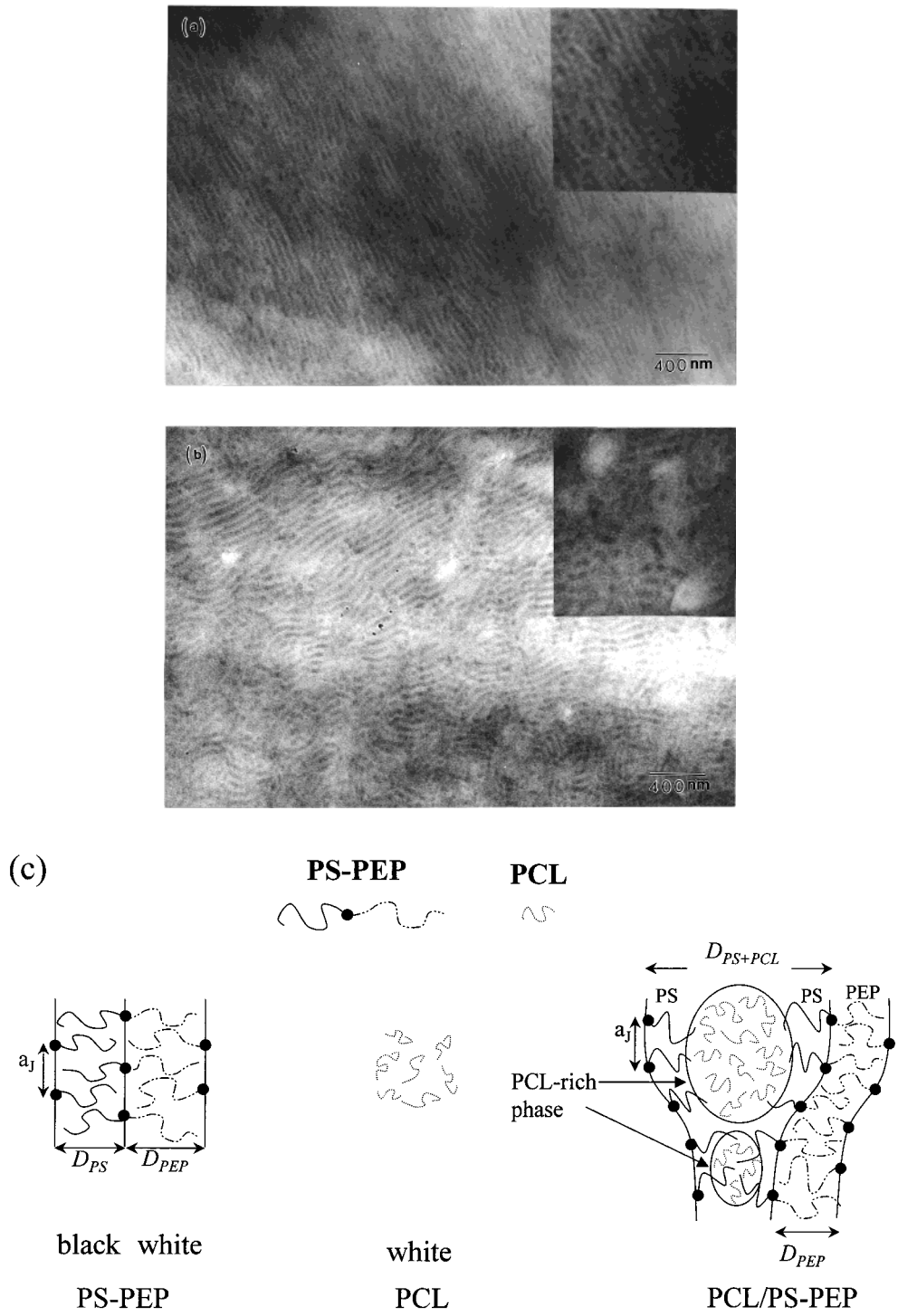


**Figure 7.** TEM micrographs of microsectioned (a) PS−PEP and (b) PCL5/PS−PEP blends by phase contrast at suitable underfocus. (c) illustrates the schematic diagram of the observed morphology. The inset shows the particular area of the micrograph at higher magnification.

effect instead of processing conditions. Further annealing thus leads to the formation of more stable state so as to boost the behavior of irregular swelling due to the localization behavior of PCL.

Many compatible systems of C/A−B blends have been studied in the past. There are also theories available to construct a phase diagram for the C/A−B systems. The theoretical works were first conducted by Hong and Noolandi[31] and then Whitmore and Noolandi.[32] Recently, random phase approximation (RPA) calculation has also been applied to determine the phase behavior of C/A−B blends.[33−37] Those compatible systems can be simply divided into two categories: one having homopolymer C possessing strong attractive interaction with either A block or B block such as the blends of SAN/PMMA−PS[37] and the other having homopolymer C possessing repulsive interaction with both A and B blocks such as PαMS/SBS blends.[30] For SAN/PMMA−PS blends, the effect of compatibilization was concluded as the result of strong attractive interaction between the SAN component and the PS block so as to inhibit the formation of macrophase separation.[37] For the PαMS/SBS blends, the solubility parameter of homopolymer PαMS is in between the values of constitu-

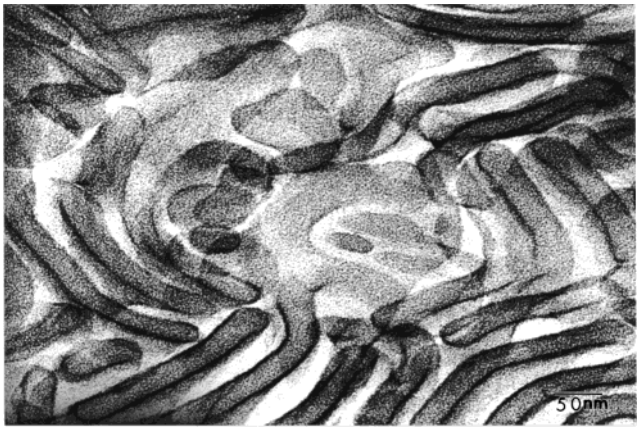


**Figure 8.** TEM micrographs of microsectioned PCL3/PS−PEP blends by mass thickness contrast after isothermal annealing at 140 °C for more than 1 week.

ent blocks of SBS. The solubility parameters of the PS block, the PB block, and the PαMS component were estimated as 9.04, 8.40, and 8.77 $(cal/cm^3)^{1/2}$, respectively, by Small's equation[25] where the densities of the PB block and the PαMS component are 0.9[27] and 1.06 $g/cm^3$.[30] It is well-known that the interaction parameter of copolymer and homopolymer may be qualitatively evaluated by the extension of classic Flory−Huggins (FH) theory.[38,39] Assuming the blends are incompressible, the modified FH theory to copolymers predicts that the effective interaction parameter, $\chi_{C/A-B}$, is a weighted average of the individual homopolymer binary interaction parameters, $\chi_{i/j}$.

$$\chi_{C/A-B} = f_A\chi_{C/A} + f_B\chi_{C/B} - f_Af_B\chi_{A/B} \quad (1)$$

where $\chi_{i/j}$ is the interaction parameter of $i$ component and $j$ component and $f_i$ is the volume fraction of constituent block $i$ for copolymer $i-j$ ($f_i + f_j = 1$). Although there are some deficiencies in the applications of this equation, the standard FH theory has led to the enormous success of the random copolymer FH type theories in explaining the enhanced miscibility observed for many systems. To justify the origins of the induced miscibility of the C/A−B blends, we simply use this equation to evaluate the correlation on the miscibility. According to the theoretical prediction of effective interaction parameter (eq 1), the relationship of interaction parameters between constituent components in blends having $\delta_A < \delta_C < \delta_B$ such as the PαMS/SBS blends are $\chi_{C/A-B} < \chi_{C/A} < \chi_{C/B}$ or $\chi_{C/A-B} < \chi_{C/B} < \chi_{C/A}$, i.e., $\chi_{P\alpha MS/SBS} < \chi_{P\alpha MS/PS} < \chi_{P\alpha MS/PB}$ due to $\delta_{PB} = 8.40$ $(cal/cm^3)^{1/2} < \delta_{P\alpha MS} = 8.77$ $(cal/cm^3)^{1/2} < \delta_{PS} = 9.04$ $(cal/cm^3)^{1/2}$. Owing to the lower value of $\chi_{P\alpha MS/SBS}$ as compared to $\chi_{P\alpha MS/PS}$ and $\chi_{P\alpha MS/PB}$, the homopolymer PαMS becomes compatible with the SBS block copolymer. Although the effects of noncombinatorial entropy and molecular factors such as their relative sizes and shapes as well as the dependence of monomer sequence are neglected in above analyses, the results in principle give a reasonable prediction with respect to the general trends for the phase behavior of the C/A−B blends.

For the PCL/PS−PEP blends, the compatibilization effect is definitely different to that of the SAN/PS−PMMA system. In contrast to the PαMS/SBS system, the solubility parameter of the PCL component ($\delta_{PCL} =$ 9.57 $(cal/cm^3)^{1/2}$) is in fact larger than both the PS block ($\delta_{PS} = 9.04$ $(cal/cm^3)^{1/2}$) and the PEP block ($\delta_{PEP} = 7.88$ $(cal/cm^3)^{1/2}$). According to the calculation, the effective interaction parameter $\chi_{PCL/PS-PEP}$ is larger than $\chi_{PCL/PS}$. It is noted that the interactions between the PCL and the constituent blocks are all repulsive (i.e., $\chi_{PCL/PEP} > \chi_{PCL/PS} > 0$). Obviously, this analyzed result is inconsistent with the experimental observations. A new mechanism for compatibilization is thus proposed in order to justify the discrepancy. We hypothesize that the advance of repulsion effect from the strongly immiscible pairs of PS/PEP and PCL/PEP makes the intrinsically immiscible pair of PCL/PS become partially miscible or compatible. The large discrepancy between the solubility parameters of the PEP block and the PS block (i.e., $\chi_{PS/PEP} \gg \chi_{PCL/PS}$) drives the PS block to favor the PCL component even though the interactions between constituent components are repulsive (i.e., $\chi_{PCL/PS} > 0$). Owing to the chemical connection between PS and PEP blocks, the formation of macrophase separation is thus restrained. Furthermore, the immiscibility between the PS block and the PCL component reduces the possibility to form well-mixed homogeneous phase. As a result, the driving force of block copolymer self-assembly (i.e., microphase separation) thus leads the PCL component to preferentially locate within the lamellar microdomains of the PS block. This new mechanism for the compatibilization of C/A−B blends is so-called the block copolymer self-assembly-induced compatibilization.

It is also interesting to find that this special phase behavior observed can be predicted by using the RPA calculation as done by Lowenhaupt and co-workers.[37] In the case of C/A−B blends where all interaction are repulsive, the calculation predicted that the phase diagram exhibits mostly microphase separation as shown in Figure 10 of ref 37. The predicted results are consistent with our morphological observations for the PCL/PS−PEP blends. However, their experimental results with respect to the blends of polycarbonate/polystyrene-*b*-poly(methyl methacrylate) (PC/PS−PMMA) were inconsistent to this predicted consequence where the macrophase separation occurs in the majority of PC/PS−PMMA blends. As a result, they suggested that the RPA model seems to be less suited for blends where all interactions are repulsive. Further studies, especially the thermodynamic derivations, are necessary to elucidate the complicated phase behavior of the compatible blends induced by the block copolymer self-assembly.

**Physically Confined Environments.** Contrary to typical microphase-separated morphology of crystallizable block copolymers,[40−54] the unique morphology having a crystallizable PCL component localized in between the lamellar microdomains of PS−PEP gives rise to a specific crystallization environment where the crystallization is carried out in nanometer-scale confined environment without the restrain of chemical connection. Since the crystallizable chain is not chemically connected to the amorphous segments, we name the assembly microstructure as physically confined system for crystalline polymer so as to distinguish the chemically confined system of crystallizable block copolymers. Having these blending microstructures allows us to obtain an integrated understanding of crystallization mechanisms within nanometer-scale environment without the effect of chemical connection. Further studies with respect to the changes on phase morphology after crystallization and the arrangement of chain folding with respect to microstructures as well as the characters

of melt and crystallization behavior for the physically confined environment are currently carried out in our laboratory.

## Conclusion

Unique self-assembly morphology of the PCL/PS−PEP blends, the irregularly swelling lamellar microdomains of the PCL component within the lamellar microdomains of the PS block and the PEP block, was observed. The formation of the PCL/PS−PEP compatible blends is suggested to be the effect of self-assembly for block copolymers. The PCL component is of favor the PS block as compared to the PEP block. Block copolymer self-assembly might be a novel approach to obtain compatible blends of homopolymer C/diblock copolymer A−B systems. Owing to the biodegradable characteristic of the PCL component, melt-blending PCL with block copolymer to form compatible blends provides a simple path to prepare biodegradable polymer blends.

**Acknowledgment.** The financial support of the National Science Council (Grant NSC 89-2216-E-005-023) is acknowledged. The authors thank Dr. H.-Y. Tsai at Union Chemical Laboratories, Industrial Technology Research Institute, for his help in melt-blending experiments. R.M.H. also thanks Dr. S. Z. D. Cheng of Institute of Polymer Science of University of Akron for his help in Synchrotron SAXS experiments and Ms. P.-C. Chao of Regional Instruments Center at NCHU for her help in TEM experiments. Our appreciation is extended to C. C. Wu and Y. S. Chen of NSYSU for assistance in X-ray measurements.

## References and Notes

(1) Doi, Y.; Koyama, N. *Macromolecules* **1996**, *29*, 5843.
(2) Liu, L.; Li, S.; Garreau, H.; Vert, M. *Biomacromolecules* **2000**, *1*, 350.
(3) Tokiwa, Y.; Ando, T.; Suzuki, T. *Ferment. Technol.* **1976**, *54*, 603.
(4) Pitt, C. G.; Gratzl, M. M.; Kimmel, G. L.; Surles, J.; Schindler, A. *Biomaterials* **1981**, *2*, 215.
(5) Potts, J. E.; Clendinning, R. A.; Ackart, W. B.; Niegisch, W. D. *Polym. Prepr.* **1972**, *13*, 629.
(6) Schindler, A.; Jeffcoat, R.; Kimmel, G. L.; Pitt, C. G.; Wall, M. E.; Zweidinger, R. In *Contemporay Topics in Polymer Science*; Pearce, E. M., Schaefgen, J. R., Eds.; Plenum: New York, 1977; Vol. 2, p 251.
(7) Chen, D. R.; Bei, J. Z.; Wang, S. G. *Polym. Degrad. Stab.* **2000**, *67*, 455.
(8) Chun, Y. S.; Kyung, Y. J.; Jung, H. C.; Kim, W. N. *Polymer* **2000**, *41*, 8729.
(9) Li, Y.; Stein, M.; Jungnickel, B.-J. *Colloid Polym. Sci.* **1991**, *269*, 772.
(10) Shabana, H. M.; Olley, R. H.; Bassett, D. C.; Jungnickel, B.-J. *Polymer* **2000**, *41*, 5513.
(11) Krause, S. In *Polymer Blends*; Paul, D. R., Newman, S., Eds.; Academic Press: New York, 1978; Vol. 1, Chapter 2.
(12) Jeon, K.-J.; Roe, R.-J. *Macromolecules* **1994**, *27*, 2439.
(13) Shull, K. R.; Winey, K. I. *Macromolecules* **1992**, *25*, 2637.
(14) Bodycomb, J.; Yamaguchi, D.; Hashimoto, T. *Macromolecules* **2000**, *33*, 5187.
(15) Winey, K. I.; Thomas, E. L.; Fetters, L. J. *Macromolecules* **1992**, *25*, 2645.
(16) Xie, R.; Li, G.; Liu, C.; Jiang, B. *Macromolecules* **1996**, *29*, 4895.
(17) Lee, S.-H.; Char, K.; Kim, G. *Macromolecules* **2000**, *33*, 7072.
(18) Hashimoto, T.; Koizumi, S.; Hasegawa, H.; Izumitani, T.; Hyde, S. T. *Macromolecules* **1992**, *25*, 1433.
(19) Spontak, R. J.; Smith, S. D.; Ashraf, A. *Macromolecules* **1993**, *26*, 5118.
(20) Winey, K. I.; Thomas, E. L.; Fetters, L. J. *Macromolecules* **1992**, *25*, 422.
(21) Koizumi, S.; Hasegawa, H.; Hashimoto, T. *Macromolecules* **1994**, *27*, 7893.
(22) Yamaguchi, D.; Shiratake, S.; Hashimoto, T. *Macromolecules* **2000**, *33*, 8258.
(23) Mayes, A. M.; Russell, T. P.; Satijia, S. K.; Majkrzak, C. F. *Macromolecules* **1992**, *25*, 6523.
(24) Ko, B.-T.; Lin, C.-C. *Macromolecules* **1999**, *32*, 8296.
(25) Small, P. A. *J. Appl. Chem.* **1953**, *3*, 71.
(26) Callaghan, T. A.; Paul, D. R. *Macromolecules* **1993**, *26*, 2439.
(27) Handlin, D. L.; Thomas, E. L. *Macromolecules* **1983**, *16*, 1514.
(28) Hashimoto, T.; Tanaka, H.; Hasegawa, H. *Macromolecules* **1990**, *23*, 4378.
(29) Tanaka, H.; Hasegawa, H.; Hashimoto, T. *Macromolecules* **1991**, *24*, 240.
(30) Kimishima, K.; Hashimoto, T.; Han, C. D. *Macromolecules* **1995**, *28*, 3842.
(31) Hong, K. M.; Noolandi, J. *Macromolecules* **1983**, *16*, 1083.
(32) Whitmore, M. D.; Noolandi, J. *Macromolecules* **1985**, *18*, 2486.
(33) Leibler, L. *Macromolecules* **1980**, *13*, 1602.
(34) Leibler, L.; Orland, H.; Wheeler, J. C. *J. Chem. Phys.* **1983**, *79*, 3550.
(35) Benoit, H.; Wu. W.; Benmouna, M.; Mozer, B.; Bauer, B.; Lapp, A. *Macromolecules* **1985**, *18*, 986.
(36) Kim, J. K.; Kimishima, K.; Hashimoto, T. *Macromolecules* **1993**, *26*, 125.
(37) Lowenhaupt, B.; Steurer, A.; Hellmann, G. P.; Gallot, Y. *Macromolecules* **1994**, *27*, 908.
(38) Stockmayer, W. H.; Moore, Jr., L. D.; Fixman, M.; Epstein, B. N. *J. Polym. Sci.* **1955**, *16*, 517.
(39) Ten Brinke, G.; Karasz, F. E.; MacKnight, W. J. *Macromolecules* **1983**, *16*, 1827.
(40) Cohen, R. E.; Cheng, P. L.; Douzinas, K.; Kofinas, P.; Berney, C. V. *Macromolecules* **1990**, *23*, 324.
(41) Nojima, S.; Kato, K.; Yamamoto, S.; Ashida, T. *Macromolecules* **1992**, *25*, 2237.
(42) Lovinger, A. J.; Han, B. J.; Padden, F. J.; Mirau, P. A. *J. Polym. Sci., Polym. Phys.* **1993**, *31*, 115.
(43) Cohen, R. E.; Bellare, A.; Drzewinski, M. A. *Macromolecules* **1994**, *27*, 2321.
(44) Rangarajan, R.; Register, R. A.; Adamson, D. H.; Fetters, L. J.; Bras, W.; Naylor, S.; Ryan, A. J. *Macromolecules* **1995**, *28*, 1422.
(45) Ryan, A. J.; Hamley, I. W.; Bras, W.; Bates, F. S. *Macromolecules* **1995**, *28*, 3860.
(46) Hamley, I. W.; Fairclough, J. P. A.; Terrill, N. J.; Ryan, A. J.; Lipic, P. M.; Bates, F. S.; Towns-Andrews, E. *Macromolecules* **1996**, *29*, 8835.
(47) Ryan, A. J.; Fairclough, J. P. A.; Hamley, I. W.; Mai, S.-M.; Booth, C. *Macromolecules* **1997**, *30*, 1723.
(48) Nojima, S.; Tanaka, H.; Rohadi, A.; Sasaki, S. *Polymer* **1998**, *39*, 1727.
(49) Balsamo, V.; Stadler, R. *Macromolecules* **1999**, *32*, 3994.
(50) Bogdanov, B.; Vidts, A.; Schacht, E.; Berghmans, H. *Macromolecules* **1999**, *32*, 726.
(51) Li, W.; Sheller, N.; Foster, M. D.; Balaishis, D.; Manners, I.; Annis, B.; Lin, J.-S. *Polymer* **2000**, *41*, 719.
(52) Park, C.; De Rosa, C.; Fetter, L. J.; Thomas, E. L. *Macromolecules* **2000**, *33*, 7931.
(53) Loo, Y. L.; Register, R. A.; Adamson, D. H. *Macromolecules* **2000**, *33*, 8361.
(54) Zhu, L.; Cheng, S. Z. D.; Calhoun, B. H.; Ge, Q.; Quirk, R. P.; Thomas, E. L.; Hsiao, B. S.; Yeh, F.; Lotz, B. *J. Am. Chem. Soc.* **2000**, *122*, 5957.

MA011381J